ResearchGate

See discussions, stats, and author profiles for this publication at: https://www.researchgate.net/publication/7437566

Quantum Chemical Investigation of Hyperfine Coupling Constants on First Coordination Sphere Water Molecule of Gadolinium(III) Aqua Complexes

ARTICLE *in* THE JOURNAL OF PHYSICAL CHEMISTRY A · JANUARY 2006

Impact Factor: 2.69 · DOI: 10.1021/jp053825+ · Source: PubMed

CITATIONS
31

READS
20

4 AUTHORS, INCLUDING:

Oleg V. Yazyev
École Polytechnique Fédérale de Lausanne
66 PUBLICATIONS **3,285** CITATIONS
SEE PROFILE

Lothar Helm
École Polytechnique Fédérale de Lausanne
240 PUBLICATIONS **7,747** CITATIONS
SEE PROFILE

Olga L Malkina
Slovak Academy of Sciences
87 PUBLICATIONS **4,231** CITATIONS
SEE PROFILE

Available from: Lothar Helm
Retrieved on: 27 January 2016

Quantum Chemical Investigation of Hyperfine Coupling Constants on First Coordination Sphere Water Molecule of Gadolinium(III) Aqua Complexes

Oleg V. Yazyev,[†] Lothar Helm,*[,†] Vladimir G. Malkin,[‡] and Olga L. Malkina[‡]

Laboratoire de Chimie Inorganique et Bioinorganique, Ecole Polytechnique Fédérale de Lausanne, EPFL-BCH, CH-1015 Lausanne, Switzerland, and Institute of Inorganic Chemistry, Slovak Academy of Sciences, SK-84536 Bratislava, Slovak Republic

Received: July 12, 2005; In Final Form: September 21, 2005

Hyperfine interactions (HFI) on the nuclei of the first coordination sphere water molecules in a model $[Gd(H_2O)_8]^{3+}$ aqua complex and in the magnetic resonance imaging contrast agent $[Gd(DOTA)(H_2O)]^-$ were studied theoretically. Density functional theory (DFT) calculations combined with classical molecular dynamics (MD) simulations have been used in order to take into account dynamic effects in aqueous solution. DFT relativistic calculations show a strong spin-polarization of the first coordination sphere water molecules. This spin-polarization leads to a positive ^{17}O isotropic hyperfine coupling constant ($A_{iso}(^{17}O) = 0.58 \pm 0.11$ MHz) and to a significant increase of the effective distance ($\langle r_{eff}(Gd-O)\rangle = 2.72 \pm 0.06$ Å) of dipolar interaction compared to the mean internuclear distance ($\langle r(Gd-O)\rangle = 2.56 \pm 0.06$ Å) obtained from the MD trajectory of $[Gd(DOTA)(H_2O)]^-$ in aqueous solution. The point-dipole model for anisotropic hyperfine interaction overestimates therefore the longitudinal relaxation rate of the ^{17}O nucleus by ∼45%. The ^1H isotropic hyperfine coupling constant of the bound water molecule is predicted to be very small ($A_{iso}(^1H) = 0.03 \pm 0.02$ MHz), and the point-dipole approximation for first coordination sphere water protons holds. The calculated hyperfine parameters are in good agreement with available experimental data.

Introduction

Hyperfine interactions (HFI), the interactions between nuclear spin and electron spin in paramagnetic systems, are of great interest for investigation of structure and dynamics in bioinorganic chemistry. The common experimental techniques that permit direct measurement of HFI are electron spin resonance (ESR), nuclear magnetic resonance (NMR), and paramagnetic relaxation enhancement (PRE) of paramagnetic systems. In the systems involving paramagnetic d-transition metal and lanthanide ions one usually separates for practical reasons the metal HFI from HFI of distant (ligand) nuclei, which are also referred to as superhyperfine interactions. A detailed study of ligand HFI in paramagnetic systems can provide researchers with a considerable amount of structural information.

As examples of the importance of the ligand HFI one can mention its decisive role in the description of NMR relaxation of solvent nuclei in solutions of paramagnetic species[1] and its impact on rational development of novel contrast agents for magnetic resonance imaging (MRI) for medical applications.[2−6] Currently, typical representatives of MRI contrast agents are gadolinium(III) complexes because of their high spin state (^8S state, half-filled f-shell) and slow electron spin relaxation. Gd(III) based MRI contrast agents are probably one of the most striking examples where the purely quantum nature of HFI directly leads to a diagnostic tool, namely, increase in contrast in an MRI image, which cannot be described by means of any kind of classical theory.

Furthermore, paramagnetic d-transition metal and lanthanide ions are used as natural and artificial probes to study structure of biological objects using experimental techniques mentioned above.[7] For instance, PRE studies of systems containing highly paramagnetic Mn^{2+} and Gd^{3+} ions can provide ultimate long-range structural constraints up to 40 Å for determination of the structure of biological objects.[1,8−11] Electron−nuclear double resonance (ENDOR) and state-of-the-art electron spin−echo envelope modulation (ESEEM) methods can locate individual nuclei in situations where it could not be done using other methods.[12,13]

It is well-known from experiment that the main contribution to the paramagnetic enhancement of longitudinal relaxation comes from dipolar contribution to HFI. The PRE for first coordination sphere water molecules is commonly described by Solomon−Bloembergen−Morgan (SBM) equations.[14−17] In the original formulation, these equations suggest the point-dipole approximation in which unpaired electrons are considered as localized at the position of the paramagnetic metal center. Any spin distribution effects over the system are therefore neglected. Due to this approximation the dipolar contribution to HFI can be described by using only information about the distance between the nucleus of interest and the nucleus of the paramagnetic center, information which can be obtained from diffraction experiments, for example. It is also worth mentioning that full knowledge of the dipolar HFI tensor is not easily accessible with existing experimental techniques and therefore the point-dipole approximation is inevitable.

Quantum chemical calculations can provide some a priori knowledge of dipolar HFI. The first step in this direction was made by Kowalewski et al.[18−20] in early studies of model aqua complexes of first row transition metal ions using the unrestricted Hartree−Fock (UHF) method. Their results clearly

* Corresponding author. Mailing address: Laboratoire de Chimie Inorganique et Bioinorganique, Ecole Polytechnique Fédérale de Lausanne, EPFL-BCH; CH-1015 Lausanne, Switzerland. Tel: +41 21 693 9876. Fax: +41 21 693 9875. E-mail: lothar.helm@epfl.ch.

[†] Ecole Polytechnique Fédérale de Lausanne.

[‡] Slovak Academy of Sciences.

10.1021/jp053825+ CCC: $30.25 © 2005 American Chemical Society
Published on Web 11/10/2005

demonstrated the limitations of the point-dipole approximation. Later UHF studies of Das et al.[21−23] and density functional theory (DFT) calculations of *Clostridium pasteurianum* iron-(III) rubredoxin protein model system by Wilkens et al.[24] confirmed this conclusion. Quantum chemical description of the system makes it possible to generalize the Solomon−Bloembergen−Morgan equations and to avoid the point-dipole approximation even at the estimative level.

The origin of ligand HFI in complexes containing a paramagnetic lanthanide ion is different from that of d-transition metal ions. Due to the core character of the f-shell any significant contribution of ligand atomic orbitals to singly occupied molecular orbitals (SOMOs) is improbable.[25] However, the effect called spin-polarization[26] may manifest in lanthanide complexes. Early studies[27] confirmed the reliability of the point-dipole approximation for spherically symmetric f^7 ions, but at that time it was not possible to apply the whole range of quantum chemistry methods available today. A more recent quantum chemical study[28] already clarified the possibility of spin-polarization effect in $Gd^{3+}-H_2O$ complexes. Nevertheless, a more detailed knowledge about the mechanisms of HFI in lanthanide complexes is required to obtain reliable parameters for structural and dynamic investigations.

In the past decade an impetuous progress in the development of quantum chemical approaches for studying HFI took place. The density functional theory (DFT) technique can now be routinely applied for investigation of HFI in model systems of hundreds of atoms in size with an accuracy approaching the experimental one.[26,29]

In the present work we study in detail both isotropic and dipolar HFI on ^1H and ^{17}O of a first coordination sphere water molecule in Gd(III) complexes. The work is composed of two parts. The first, methodological part serves for the validation of DFT as an accurate tool for description of HFI in lanthanide complexes where the amount of reliable experimental data concerning hyperfine coupling constants is limited. Keeping in mind that relativistic effects play an important role for heavy element compounds we use state-of-the-art relativistic theory all-electron approaches. A simple symmetric system modeling the Gd^{3+} octaaquaion is used for this first part. The second part considers the HFI on the first coordination sphere water molecule of the $[Gd(DOTA)(H_2O)]^-$ complex. This chelate complex is a typical member of the family of Gd^{3+} complexes which are actually used in medical applications as MRI contrast agents. To take into account the dynamic nature of the complex in aqueous solution as well as to investigate the influence of geometric parameters such as the ion−water distance on HFI, we use an approach which combines classical MD simulations with quantum chemistry calculations of HFI. The main purpose of this work is to show the limitations of point-dipole approximation for dipolar contributions to HFI of first coordination sphere water molecules in Gd(III) complexes and to propose corrections if possible. The deep understanding of underlying physical phenomena in this class of chemical compounds is a necessary element for future development of effective MRI contrast agents for medical and other applications.

The outline of the article is as follows: First we review the definitions and models of hyperfine interactions and nuclear relaxation in the section Theoretical Foundation. Then the choice of model systems and details of quantum chemistry methods are explained in the section Computational Techniques. In the next section, Results and Discussion, the performance of the applied computational methods is discussed. The calculated ligand hyperfine parameters and the phenomenon of spin-polarization for model Gd^{3+} octaaqua complex and more realistic $[Gd(DOTA)(H_2O)]^-$ in solution are also considered. The predicted constants are compared with the existing experimental data. In the last subsection, the conclusions for evaluation of relaxation data are made.

Theoretical Foundation

Hyperfine interactions are magnetic interactions between nuclear and electron spins. The corresponding spin-Hamiltonian of this interaction can be written as

$$\mathbf{H} = \mathbf{S}\cdot\mathbf{A}\cdot\mathbf{I} \tag{1}$$

where $\mathbf{A}$ is the 3×3 HFI tensor and $\mathbf{S}$ and $\mathbf{I}$ are the vectors of the electron and the nuclear spin, respectively. The HFI tensor can be split into isotropic and anisotropic parts,

$$\mathbf{A} = A_{\mathrm{iso}}\mathbf{1} + \mathbf{T} \tag{2}$$

where A_{iso} is the isotropic hyperfine coupling constant (scalar); $\mathbf{1}$ is the 3×3 unit matrix, and $\mathbf{T}$ is the traceless matrix of the anisotropic contribution. Within the commonly used Breit−Pauli approximation,[30] the scalar isotropic (Fermi contact) hyperfine coupling constant on nucleus N is

$$A_{\mathrm{iso}}(\mathrm{N}) = \frac{4\pi}{3S}\beta_e\beta_N g_e g_N \rho^{\alpha-\beta}(\mathbf{R}_N) \tag{3}$$

and a matrix element of the anisotropic (dipolar) contribution is

$$T_{ij}(\mathrm{N}) = \frac{1}{2S}\beta_e\beta_N g_e g_N \int \rho^{\alpha-\beta}(\mathbf{r}) \times \frac{(\mathbf{r}-\mathbf{R}_N)^2\delta_{ij} - 3(r_i - \mathbf{R}_{Ni})\cdot(r_j - \mathbf{R}_{Nj})}{(\mathbf{r}-\mathbf{R}_N)^5}\mathrm{d}\mathbf{r} \tag{4}$$

where β_e and β_N are Bohr and nuclear magnetons, respectively, g_e and g_N are free-electron and nuclear g-values, and S is the total electronic spin of the atom, ion, or molecule. Thus, both contributions depend only on the distribution of the electron spin density, the difference between majority spin (α) and minority spin (β) densities, $\rho^{\alpha-\beta}(\mathbf{r}) = \rho^{\alpha}(\mathbf{r}) - \rho^{\beta}(\mathbf{r})$, of the system in the spin state S and physical constants.

The physical interpretations of the two contributions to $\mathbf{A}$ are as follows. The isotropic contribution (Fermi contact), A_{iso}, is proportional to the value of the spin density at the position of nucleus N and thus it possesses a local character. Physically this contribution represents a magnetic field generated at the point of nucleus by the presence of the electron magnetic moment itself. On the contrary, the anisotropic contribution, $\mathbf{T}$, is the dipolar integral over the whole space and has therefore a nonlocal character. It represents the dipole−dipole type of magnetic interaction between the magnetic moments of nuclear and electron spins. The dipolar contribution vanishes if the spin density is highly symmetric when observed from the point of nucleus N.

In many cases the spin density distribution is determined by the shapes of singly occupied molecular orbitals (SOMOs). This contribution is usually referred to as spin-delocalization and it is always positive, if one follows the above-mentioned convention for α- and β-electron densities. A second part of spin density comes from so-called spin-polarization effects, which originate from nonequal potentials experienced by α and β electrons and orthogonality constraints imposed on MOs: this leads to different shapes of α and β MOs (which otherwise would be doubly occupied). This contribution can be positive as well as

negative at the location of nucleus N, but it always integrates to zero. Spin-polarization effects can be described in short as "an effective attraction": the localized unpaired electrons "attract" the nearby ones of the same spin. This can result in a negative spin density in the vicinity of SOMO nodes and where SOMO density is vanishing and in a slight increase of positive spin density, produced by the spin-delocalization effect. Spin-polarization is often referred to as a second-order effect.[31] The superposition of these two effects will be referred to as spin-distribution from now on.

In chemical systems involving paramagnetic metal ions it is common to separate the notions of hyperfine coupling constants on the metal nucleus and on ligand nuclei. In this work we discuss only ligand hyperfine interactions which are often referred to as superhyperfine coupling. The simplest possible model for ligand HFI is the point-dipole approximation.[20] Within this approximation spin-distribution effects are neglected and the dipolar ligand HFI tensor $\mathbf{T}^{PD}$ depends only on the distance between the metal and ligand nuclei, r_{MX}. Thus, $\mathbf{T}^{PD}$ can be written in form[32]

$$\mathbf{T}^{PD} = \beta_e\beta_N g_e g_N \frac{1}{r_{MX}^3}\begin{pmatrix} 2 & 0 & 0 \\ 0 & -1 & 0 \\ 0 & 0 & -1 \end{pmatrix} \quad (5)$$

assuming that the metal−ligand nucleus vector is (r_{MX}, 0, 0). It is also worth mentioning that this approximation results in a zero isotropic hyperfine coupling constant on all ligand nuclei since all the spin density is located on the metal ion. Thus, nonzero ligand isotropic hyperfine coupling constants (which are often experimentally measurable) tell us immediately about the deficiency of the point-dipole approximation. The sign of the ligand hyperfine coupling constant provides the sign of the spin density at the position of ligand nuclei and thus gives the important information about the relative magnitude of spin-delocalization and spin-polarization effects.

Hyperfine interaction results in a shift of NMR resonance frequency and in an enhancement of nuclear spin relaxation. The SBM equations[14−17] describe the increase of longitudinal, $1/T_1$, and transverse, $1/T_2$, relaxation rates of ligand nuclei in the inner coordination sphere of a paramagnetic complex due to the time-dependent interaction with the electron spin. As in the general case of hyperfine interactions, relaxation rates can also be split into a scalar (Fermi contact) $1/T_i^{SC}$ and a dipolar $1/T_i^{DD}$ contribution,

$$\frac{1}{T_1^{SC}} = \frac{2S(S+1)}{3}\left(\frac{A}{\hbar}\right)^2\left[\frac{\tau_{s2}}{1+\omega_S^2\tau_{s2}^2}\right] \quad (6)$$

$$\frac{1}{T_2^{SC}} = \frac{S(S+1)}{3}\left(\frac{A}{\hbar}\right)^2\left[\frac{\tau_{s2}}{1+\omega_S^2\tau_{s2}^2} + \tau_{s1}\right] \quad (7)$$

$$\frac{1}{T_1^{DD}} = \frac{2}{15}\frac{(\beta_e\beta_N g_e g_N)^2}{r_{MX}^6}S(S+1)\left(\frac{\mu_0}{4\pi}\right)^2\left[7\frac{\tau_{d2}}{1+\omega_S^2\tau_{d2}^2} + 3\frac{\tau_{d1}}{1+\omega_I^2\tau_{d1}^2}\right] \quad (8)$$

$$\frac{1}{T_2^{DD}} = \frac{1}{15}\frac{(\beta_e\beta_N g_e g_N)^2}{r_{MX}^6}S(S+1)\left(\frac{\mu_0}{4\pi}\right)^2\left[13\frac{\tau_{d2}}{1+\omega_S^2\tau_{d2}^2} + 3\frac{\tau_{d1}}{1+\omega_I^2\tau_{d1}^2} + 4\tau_{d1}\right] \quad (9)$$

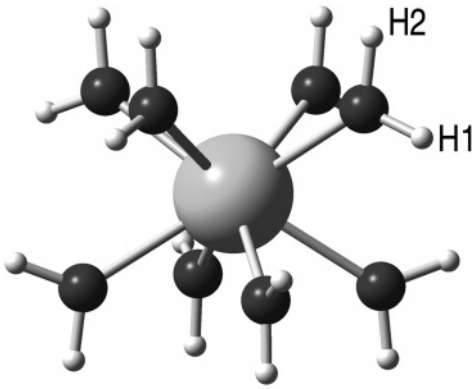

Figure 1. The structure of the model Gd^{3+} octaaqua complex of D_{4d} symmetry. The 4-fold symmetry axis is aligned to be vertical.

where ω_S and ω_I are the electron and nuclear Larmor frequencies in rad s^{-1}, r_{MX} is the distance between the nucleus of the paramagnetic ion and the ligand nucleus under observation, and τ_{si} and τ_{di} are characteristic correlation times of scalar and dipolar relaxation processes which in turn depend on the correlation times of molecular rotation, τ_R, on the residence time of the ligand in the inner coordination sphere of the paramagnetic ion, τ_M, and on electron spin relaxation times, T_{1e},T_{2e}. Note that $A/\hbar$ in SBM equations is equal to $2\pi A_{iso}$ as defined in eq 3.

Once the principal values (two independent parameters) of the dipolar HFI tensor **T** are known (from quantum-chemical calculations, for example), it is possible to overcome the point-dipole approximation and to rewrite the "HFI factor" in the dipolar SBM equations in a generalized form introducing the notation of an "effective" distance r_{eff}[18−20] for the dipole−dipole interaction,

$$r_{eff} = \left(\frac{S}{\beta_e\beta_N g_e g_N}\right)^2\left[T_{zz}^2 + \frac{1}{3}(T_{xx} - T_{yy})^2\right]^{-1/6} \quad (10)$$

where T_{zz} is the maximal absolute value of the principal components of the dipolar HFI tensor and T_{xx}, T_{yy} are the other two eigenvalues of **T**.

Because of the $1/r^3$ dependence of dipolar interactions, even small spin-distribution effects on the ligand nucleus can significantly influence the resulting value of the effective distance of the dipolar hyperfine interaction. For relaxation rates, this dependence is even stronger since HFI enter in square in eqs 6−9 thus resulting in $1/r^6$ dependence. It is therefore useful to decompose the dipolar HFI into a point-dipole and a ligand-centered contribution:

$$\mathbf{T} = \mathbf{T}^{PD} + \mathbf{T}^{LC} \quad (11)$$

Several simplifications have been proposed in the literature for the analysis of ligand-centered contributions.[33−35] However, all these models were intrinsically linked to specific chemical systems. The approach presented below is free from specific approximations and still provides a clear insight into relations between the dipolar HFI tensor and $\mathbf{T}^{PD}$.

Computational Techniques

Model Systems. In this work we present a two-stage computational strategy to calculate dipolar HFI tensors. In the first stage, we studied as model compound $[Gd(H_2O)_8]^{3+}$ with a square antiprismatic coordination polyhedron of D_{4d} symmetry (Figure 1). The geometry of the system is the same as described by Borel et al. [36] except for the Gd−O distance which was fixed

to 2.40 Å for the sake of better agreement with experimental studies[37] of Gd^{3+} in aqueous solution. Due to the small size and the high symmetry of the aquaion, quantum chemical calculations of the complex are rather undemanding. That allowed us to perform a very detailed study of the influence of the basis set quality as well as other computational aspects on the HFI tensor.

The second stage involves a study of the $[Gd(DOTA)(H_2O)]^-$ complex in aqueous solution. To take into account solvent effects and to provide sufficient statistical averaging of the calculated HFI tensor we used a cluster method (see Chapter 11 in ref 26 and references therein). This approach implies the ensemble averaging of a property calculated for a set of single configurations (often referred to as "snapshots") extracted from a molecular dynamics simulation trajectory. This approach has been proven to be reasonable for studying properties such as NMR chemical shifts,[38] nuclear quadrupolar coupling constants,[39−42] hyperfine coupling constants,[43] and **g**-tensors[44] of fluids and biosystems in solution. In our work, we applied this approach to investigate an extended system including almost 100 atoms with the focus on the Gd^{3+} ion in the complex and on the water molecule directly bound to it.

A classical molecular dynamics simulation of the $[GdDOTA(H_2O)]^-$ complex in water has been performed in a periodic box containing the complex anion, Jorgensen TIP3P water molecules,[45] and a Na^+ counterion using *Amber 6.0* code[46] ($T = 300$ K, $P = 1$ atm, NPT ensemble). The parametrization of $[GdDOTA(H_2O)]^-$ and the details of the simulation have been described previously.[47,48] It is known from experiment that the $[GdDOTA(H_2O)]^-$ complex is present in solution as a mixture of major ***M*** (80%) and minor ***m*** (20%) conformers with different coordination polyhedra and ligand conformations.[49] Only the major ***M*** isomer has been simulated and was therefore considered in the present study. The configuration space sampling (100 snapshots) was extracted from the trajectory at regular intervals of 10 ps. The time series of geometric parameters and calculated properties show no autocorrelation. The single configuration (cluster) for quantum chemical calculations consisted of the $[GdDOTA(H_2O)]^-$ complex and the 6 second sphere water molecules closest to the inner sphere water molecule (74 atoms in total). Including second sphere water molecules ensures an adequate treatment of close-range solvent effects. Moreover, using the polarizable continuum model (PCM) calculations, we found that far-range solvent effects do not significantly influence the hyperfine coupling constants of the first coordination sphere water molecule. We neglected therefore in our quantum chemical calculations long-range solvent effects, and all calculations were performed for isolated clusters chosen from the snapshots. A typical example of a single configuration is shown in Figure 2.

Theoretical Methods. Calculations of lanthanide compounds as well as those of other heavy elements require an adequate treatment of relativistic effects.[50] In general, there are a few alternative ways to treat relativistic effects. Usually one has to chose between all-electron treatment (including only scalar or both scalar and spin−orbit relativistic effects) and relativistic effective core potentials (RECP), which themselves can also be pure scalar or include as well the spin−orbital part. The use of RECP can significantly reduce computational efforts since core electrons are removed and replaced by an effective operator. Several RECP parametrizations for gadolinium[51,52] are available for routine applications. These pseudopotentials were proven to reproduce reliably experimental molecular geometries and vibrational spectra of gadolinium compounds.[53,54] However, we found that for HFI tensor calculations all-electron treatments are much better than RECP approaches we considered.[55] Therefore, in the following we will only discuss the results of all-electron approaches.

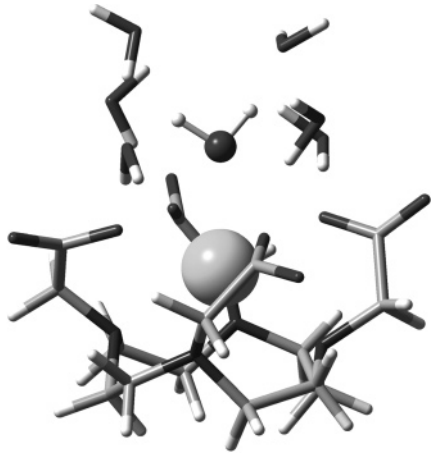

Figure 2. A typical "snapshot" extracted from MD simulation of $[GdDOTA(H_2O)]^-$. The Gd^{3+} ion and first coordination sphere water molecule are shown in balls and sticks; the polyaminocarboxylate ligand DOTA and 6 second coordination sphere water molecules are presented as tubes.

Currently, among the all-electron relativistic approaches the family of Douglas−Kroll−Hess (DKH) transformation[56] based methods and zero order regular approximation (ZORA)[57−59] are the methods most widely tested and used. In a first stage of our computational study we compare second order Douglas−Kroll−Hess method (DKH2) implemented in the *Gaussian03* suite of programs[60] with the ZORA method available in *ADF2003* package.[61] For consistency the point-nucleus model was used in both methods (this is a good approximation in the present study since we are interested in HFI tensors on ligand nuclei only). Spin−orbit coupling terms were not taken into account since they were not expected to be important for HFI tensor calculations due to the electronic structure and the high coordination (8 or 9) of Gd^{3+} in the compounds under study. In addition, recent calculations of spin−orbit corrections to HFI tensor for lighter nuclei found only minor effects.[62,63]

The choice of basis set becomes a nontrivial task if one considers calculations of isotropic hyperfine coupling constants. There are two main problems associated with basis sets in such calculations. First, the accurate representation of nuclear cusp is necessary for evaluation of spin density at the point of nucleus. While this can be naturally covered using Slater type orbital (STO) basis sets, extra tight exponents are needed for Gaussian type orbital (GTO) basis sets. Second, it is not feasible to use large contractions (in the case of GTO basis sets) for the description of the core region because the additional flexibility is required to take into account spin-polarization effects.[64,65] Therefore, the core basis functions have to be considerably uncontracted if GTO basis sets are used or simply represented by a sufficient number of functions of STO basis sets. The frozen core approximation is unacceptable in calculations of HFI if the core MOs are frozen on the nucleus of interest. In the present study, we used both GTO and STO basis sets for the calculations of the model Gd^{3+} octaaqua complex. The GTO set used in all DKH2 calculations was composed from relativistic basis sets (Hirao et al.[66]) by complete uncontraction and, in addition, for the light atoms, it was augmented with the polarization functions from the IGLO-III basis set.[67] In ZORA calculations on $[Gd(H_2O)_8]^{3+}$ we used the standard TZ2P STO basis set from the ADF package. However, here the concept of basis set "of

high local quality" [68] (locally dense basis set) was used in order to reduce the amount of computational resources required. In our case the TZ2P basis set was used only for the part of interest, Gd^{3+} and first coordination sphere water molecules, while the rest of the system was treated using the DZ basis set with frozen 1s core. On Gd the frozen core up to the 4d shell was used while no frozen core approximation was employed for the atoms of first coordination sphere water molecules. Using model calculations we showed that this approximation does not affect superhyperfine coupling constants on the ligand nuclei.

While most quantum chemical calculations are nowadays performed with the DFT approach, the question about its performance in calculations of a particular property is not an easy one. DFT for calculations of HFI of organic radicals gives acceptable results, and good accuracy can be achieved with pure density functionals except for some pathological cases. However, transition metal complexes are much more difficult to calculate, and some pictorial failures of pure density functionals are known.[69] For instance, DFT tends to overestimate the coordination bond covalency in Cu^{2+}, which in turn leads to a more delocalized character of SOMO in such systems. Moreover, there is no a priori known best exchange-correlation functional for calculation of hyperfine coupling constants: all GGA functionals behave more or less similarly while hybrid density functionals usually give better results.[64,69] The use of hybrid density functionals (especially with a large admixture of HF exchange) increases, however, spin contamination, which could lead to inferior results.[64] The electronic structure of lanthanide compounds differs significantly from d-transition metal complexes: the core character of unpaired f-shell electrons makes an admixture of excited states energetically unfavorable. Thus, in principle, an admixture of the Hartree−Fock exchange should not lead to severe spin-contamination. The question about the performance of DFT for the description of spin-polarization driven effects on HFI tensor in lanthanides is still unexplored, and we present here a first attempt of such benchmark calculations. Among available exchange-correlation density functionals the exchange functional of Becke[70] and the correlation functional of Perdew and Wang[71] (this combination is known as the BPW91 functional) were chosen relying on benchmark calculations from Kaupp et al.[64] Thus we used BPW91 as a pure DFT functional, B3PW91[72] as its hybrid modification, and the Hartree−Fock method for completeness of the consideration. All methods were used in their spin-unrestricted implementation necessary to take into account spin-polarization effects.

In all calculations performed with the *Gaussian03* package the tight SCF convergence criterion (*SCF=tight* keyword) and fine numerical integration grids (*Integral(FineGrid)* keyword) have been used. The use of symmetry in the evaluation and storage of integrals was disabled. In *ADF2003* calculations the numerical integration parameter of 6.0 was used (*Integration 6.0* keyword). We proved that using higher convergence criteria and more accurate integration grids does not influence values of calculated HFCCs. The calculations were performed on a homemade PC cluster.

Results and Discussion

Validation of Methodology of Quantum Chemical Calculations. The detailed calculations on the small model $[Gd(H_2O)_8]^{3+}$ allowed us to assess the reliability of density functional theory calculations of HFI for Gd complexes. The obtained isotropic ^{17}O hyperfine coupling constants (HFCC) (Table 1) are between 0.61 and 1.02 MHz for the DFT calculations. An admixture of the HF exchange to the exchange-correlation potential (B3PW91 vs BPW91) pushes the calculated ^{17}O HFCC in the direction of the HF results, which is not unexpected. The difference between ZORA and DKH results for isotropic ^{17}O HFCC can be attributed to the neglect of so-called picture-change effect in present DKH calculations.[73] Taking into account that, due to a very local character of the Fermi contact operator, the isotropic constants are very difficult to evaluate computationally, the results show reasonable mutual agreement. Furthermore, the DFT calculations are consistent with the experimental values of 0.84 MHz[74,75] and 0.71 MHz[76] for $[Gd(H_2O)_8]^{3+}$. Our model calculations do not include long-range solvent effects which are expected to be insignificant for HFI. Therefore, both pure and hybrid density functionals look reliable to describe ligand nuclei HFI in the compounds studied. The positive isotropic HFCC, A_{iso}, on ^{17}O nuclei corresponds to a negative spin-density at the point of the O nucleus of -0.0118 au^{-3} while the most negative value of spin-density within cross sections shown in Figure 3 is -0.1342 au^{-3}.

The calculated T_{zz} values (Table 1) of the ^{17}O HFI anisotropy tensor are noticeably lower (about -1.35 MHz) than predicted by the point-dipole approximation (-1.55 MHz) using eq 5 and $r_{Gd-O} = 2.40$ Å. All quantum chemical methods used in this study give results in good mutual agreement, which is not surprising since it is well-known that HFI anisotropy is much

TABLE 1: Calculated ^{17}O and ^{1}H Hyperfine Tensors for the First Coordination Sphere Water Molecules of the $[Gd(H_2O)_8]^{3+}$ Model System[a]

method	A_{iso}, MHz	T_{xx}, MHz	T_{yy}, MHz	T_{zz}, MHz	r_{eff}, Å
		^{17}O			
BPW91/ZORA/TZ2P	0.61	0.802	0.560	−1.362	2.50
BPW91/DKH2/Hirao	0.78	0.761	0.583	−1.344	2.51
B3PW91/DKH2/Hirao	1.02	0.716	0.633	−1.349	2.51
HF/DKH2/Hirao	1.60	0.681	0.671	−1.352	2.51
exptl/point-dipole[b]	0.84	0.775	0.775	−1.551	2.40
		^{1}H			
BPW91/ZORA/TZ2P	0.022	−2.652	−2.625	5.277	3.105
	0.028	−2.651	−2.626	5.277	3.106
BPW91/DKH2/Hirao	−0.001	−2.655	−2.623	5.278	3.105
	0.009	−2.653	−2.623	5.275	3.106
B3PW91/DKH2/Hirao	−0.031	−2.666	−2.618	5.283	3.104
	−0.023	−2.663	−2.618	5.281	3.105
HF/DKH2/Hirao	−0.044	−2.677	−2.606	5.283	3.104
	−0.029	−2.674	−2.607	5.280	3.105
exptl/point-dipole[b]	0.03 ± 0.02	−2.643	−2.643	5.287	3.1037

[a] Two different values for ^{1}H correspond to two types of protons a in the model system. H1 and H2 protons as shown in Figure 1 belong to the same water molecule and are equivalent for different water molecules. H1 protons are equatorial and H2 are axial with respect to the symmetry axis. The Gd−H1 and Gd−H2 distances are equal. [b] r_{eff} obtained using the point-dipole approximation.

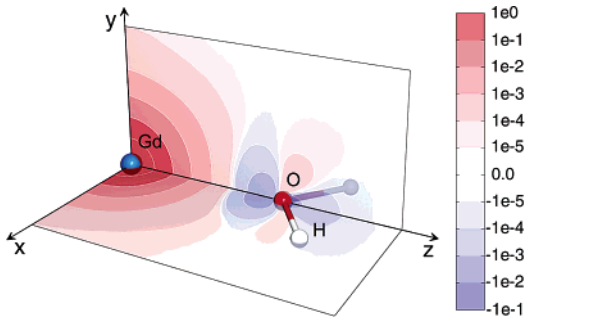

Figure 3. Spin density map of the $[Gd(H_2O)_8]^{3+}$ model system (calculated at the BPW91/DKH2/Hirao level of theory, in au^{-3}) shows the Gd^{3+} ion and one of the water molecules. Cross sections of size 2 × 4 Å in XOZ and YOZ planes are shown.

less sensitive to the computational aspects than the isotropic part.[26] Again this excellent agreement supports our confidence in using the DFT method in the calculations of HFI on ligand nuclei in lanthanide compounds. The rhombicity of HFI anisotropy tensor, $T_{xx} - T_{yy}$, depends on the choice of quantum chemical method. The pure density functional BPW91 yields the largest positive $T_{xx} - T_{yy}$ values (0.242 and 0.178 MHz) as a consequence of possible residual π-binding involving f-electrons. This is not surprising since pure density functionals are known to overestimate the covalency of coordination bond. However, for Gd^{3+} the rhombicity influences only slightly the effective distance r_{eff} (eq 10), which is almost solely defined by the T_{zz} value. Our calculations of the HFI anisotropy tensor are in qualitative agreement with the estimations of Raitsimring et al.[77] In their calculations they estimate the spin population of the whole $s-p_z$ hybrid orbital of the O atom from the experimental isotropic ^{17}O HFCC and neglect any valence shell and core shell spin-polarization effects. We have shown recently that these effects might be significant and can be taken into account within quantum chemical calculations.[78]

The calculated ^1H isotropic hyperfine couplings are very small (Table 1). The increase of amount of exact exchange tends to decrease spin density at ^1H nucleus and even to change its sign. This can be attributed to the fact that the hydrogen atoms lie very close to a node of the spin-density surface (see Figure 3). The calculated ^1H HFI anisotropy tensors are in very good agreement with each other and with the point-dipole approximation. All tested quantum chemistry methods give a negligible ligand-centered contribution to the ^1H HFI tensor.

The basis sets used in our calculations are sufficient since calculated HFCC's do not show significant changes upon the addition of extra basis functions. The purity of spin states is proven by calculated $\langle S^2 \rangle$ values (for DFT methods we use Kohn−Sham determinant to evaluate $\langle S^2 \rangle$). For BPW91, B3PW91, and HF calculations with GTO basis set the calculated values of $\langle S^2 \rangle$ are 15.7556, 15.7556, and 15.7576, correspondingly, while the nominal value for a pure octet state is 15.75.

Hyperfine Coupling Constants of ^{17}O and ^1H in $[Gd(H_2O)_8]^{3+}$. The qualitative inspection of spin density maps presented graphically in Figure 3 shows the strong spin-polarization effect on the water molecule. While most of the positive spin density resides on the Gd^{3+} ion itself, electron density along Gd−O bond is significantly spin-polarized, leading to two important consequences.

First, the calculated T_{zz} value (OZ axis is oriented along Gd−O bond) of −1.35 MHz for ^{17}O (Table 1) is noticeably lower than the value of −1.55 MHz predicted by the point-dipole approximation (eq 5). This reduction of the T_{zz} value leads to an effective distance of $r_{eff} = 2.50$ Å for the dipole−dipole interaction (eq 10), which is considerably longer than the Gd−O internuclear distance $r_{Gd-O} = 2.40$ Å (Table 2). One can think about this effect as a partial compensation of magnetic dipole−dipole interaction between the positive spin-density on the Gd^{3+} ion and the ^{17}O nucleus by the negative spin-density induced on the ligand. Furthermore, it is interesting to note the positive spin density located in the YOZ plane perpendicular to the plane of the water molecule (Figure 3). This is reflected in the bigger value of $T_{xx} - T_{yy}$ for BPW91 calculations and can be a consequence of some residual π-binding involving f-electrons or a spin alternation effect. However, as it was discussed above, the small rhombicity of the oxygen HFI anisotropy tensor almost does not influence the resulting value of the effective distance of dipolar interaction r_{eff}(Gd−O).

TABLE 2: Comparison of Calculated (BPW91/ZORA/TZ2P) and Experimental Hyperfine Interaction Parameters for $[Gd(H_2O)_8]^{3+}$ and $[Gd(L)(H_2O)]^{n-}$ [a]

	$[Gd(H_2O)_8]^{3+}$		$[Gd(L)(H_2O)]^{n-}$	
	calcd	exptl	calcd[b]	exptl
		^{17}O		
r_{Gd-O}, Å[c]	2.4		2.56 (0.06)	
r_{eff}, Å[d]	2.50		2.72 (0.06)	
A_{iso}, MHz	0.61	0.79[e]	0.58 (0.11)	0.59[h]
		0.84[f]		0.75[i]
		0.75[g]		
T_{xx}, MHz	0.802	0.76[g,l]	0.623	0.76[i]
T_{yy}, MHz	0.560	0.62[g,l]	0.452	0.62[i]
T_{zz}, MHz	−1.362	−1.38[g]	−1.061 (0.09)	−1.38[i]
		^1H		
r_{Gd-H}, Å	3.1037		3.27 (0.14)	
r_{eff}, Å	3.106	3.09[j]	3.27 (0.14)	3.06[i]
A_{iso}, MHz	0.025	0.04[e]	−0.032 (0.08)	−0.04[k]
		0.03[j]		
T_{xx}, MHz	−2.652	−2.67[j]	−2.306	−2.75[k]
T_{yy}, MHz	−2.626	−2.67[j]	−2.256	−2.75[k]
T_{zz}, MHz	5.277	5.34[j]	4.562 (0.66)	5.5[k]

[a] The distribution widths from molecular dynamics sampling are given in parentheses. [b] L = DOTA. [c] Nuclear distance. [d] Effective distance of dipole−dipole interaction. [e] From NMR chemical shift (ref 76), corrected for coordination number of 8. [f] From NMR chemical shift (ref 75). [g] From ENDOR experiments (ref 80). [h] L = DOTA, NMR chemical shift (ref 75). [i] L = MS-325, ENDOR experiments (ref 77). [j] From ENDOR (ref 80). [k] L = HPDO3A, ENDOR experiments (ref 80). [l] From the estimated rhombicity of 0.14 MHz for the planar model 2 (ref 77).

Second, the ^{17}O isotropic hyperfine coupling constant, A_{iso}, is positive as the consequence of a negative spin density at the oxygen nucleus and the negative magnetic moment of the ^{17}O nucleus. As we already mentioned in the beginning of this section, the experimental values of 0.71 MHz[76] and 0.84 MHz[74] lie within the 0.61−1.02 MHz range of DFT predictions (Table 1).[79] The magnitude of the coupling is relatively small since the $s-p_z$ hybrid atomic orbital of O, which is mostly affected by spin-polarization, has little of s-character and therefore its node lies very close to the nucleus.

The Gd−H effective distance of dipole−dipole magnetic interaction recalculated via data of quantum chemical calculations (Table 2) is only slightly bigger than the distance between the nuclei, r_{Gd-H}. The point-dipole approximation is therefore valid for hydrogens of water molecules in $[Gd(H_2O)_8]^{3+}$. The validity of this approximation for ^1H has already been found in a previous study on dipolar HFI in d-transition metal aquaions.[19] The rationalization of this observation is that p-type atomic orbitals on hydrogen play only a minor role in bonding (and thus could not contribute significantly to the anisotropy of the HFI tensor) whereas the s-type atomic orbital gives zero contribution to the anisotropy of the tensor (but determines the isotropic constant A_{iso}).

The calculated ^1H isotropic hyperfine couplings are close to zero and in good agreement with experimental data. For instance, single-crystal EPR studies[80] put this value between −0.015 and +0.04 MHz while the most reliable ENDOR[81] gives $+0.03 \pm 0.02$ MHz. Bryden et al.[82] deduced ^1H HFCC from NMR data to be about 0.005 MHz. We conclude that there is rather large uncertainty in the experimental data due to the small absolute magnitude of the coupling.

Isotropic Hyperfine Coupling Constants of ^{17}O and ^1H in $[Gd(DOTA)(H_2O)]^-$. The isotropic ^{17}O HFCCs obtained using the DFT cluster approach with averaging over a set of snapshots selected from a classical molecular dynamic simulation are in

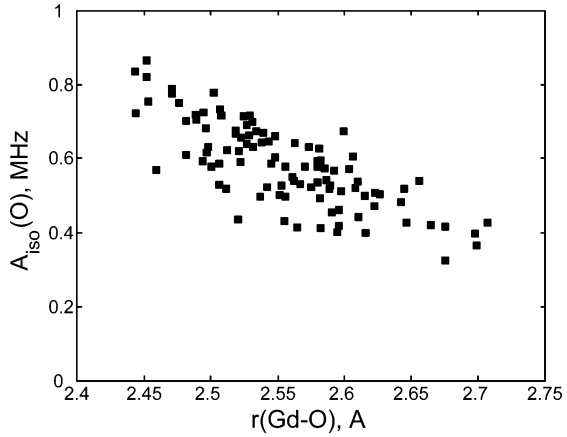

Figure 4. ^{17}O isotropic hyperfine coupling constant, A_{iso}, plotted as function of Gd−O distance for 100 configurations extracted from MD trajectory of $[Gd(DOTA)(H_2O)]^-$.

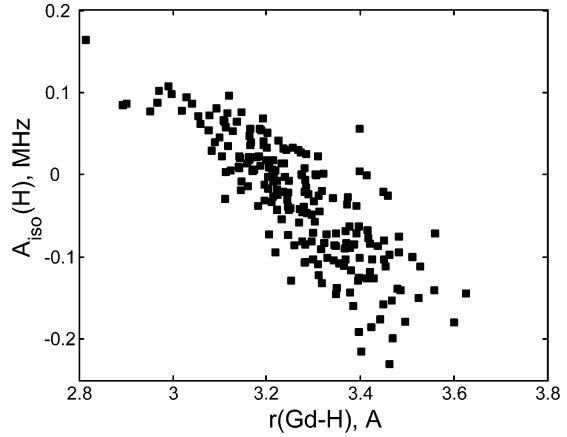

Figure 5. ^{1}H isotropic hyperfine coupling constant plotted as function of Gd−H distance for 100 configurations (200 values totally) extracted from MD trajectory.

a very good agreement with experimental data. A major parameter influencing the ^{17}O HFCC is the Gd−O distance, r_{Gd-O}, which fluctuates during the molecular dynamics simulation. Figure 4 shows the isotropic hyperfine coupling constant as a function of r_{Gd-O}. The averaged A_{iso}(O) is 0.58 MHz (standard deviation: 0.11 MHz) for an average distance of 2.56 ± 0.06 Å; that is in excellent agreement with the value of 0.59 ± 0.03 MHz determined from ^{17}O NMR chemical shift data.[75] In all geometric configurations obtained from the snapshots the spin density at the position of oxygen nucleus is negative in accord with the spin polarization mechanism. The magnitude of A_{iso}(O) strongly correlates with the Gd−O distance and the spin-polarization effect decays rapidly with the increase of r_{Gd-O}. The mean Gd−O distance from the classical MD simulation is however about 0.1 Å longer than that of the solid-state X-ray[83] or the solution XAFS structure.[84] ^{17}O electron nuclear double resonance spectra of the MS-325, a Gd^{3+} complex with an acyclic ligand, recorded in frozen solution, gave spectra of a shape similar to that of the Gd^{3+} aquaion.[77] The authors concluded therefore that the ^{17}O hyperfine coupling parameters of both complexes are the same, $A_{iso} = 0.75$ MHz.

The calculated mean value of the ^{1}H isotropic hyperfine coupling constant (−0.032 ± 0.08 MHz) is very small and varies from about −0.2 to + 0.1 MHz (Figure 5). Again a strong correlation with the Gd−H distance is observed. The corresponding NMR experimental value of Bryden et al.[82] for $[Gd(DOTA)(H_2O)]^-$ is about 0.075 MHz while the two-dimensional Mims ENDOR result[81] for $[Gd(HP\text{-}DO3A)(H_2O)]^-$

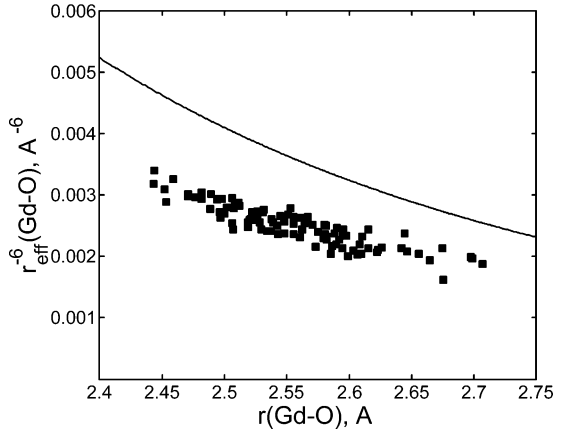

Figure 6. The r_{eff}^{-6}(Gd−O) factor for the oxygen atom of bound water in $[GdDOTA(H_2O)]^-$ obtained from eq 10 based on the calculated dipolar HFI tensors of the 100 MD "snapshots". The line corresponds to r^{-6}(Gd−O) calculated using the point-dipole approximation.

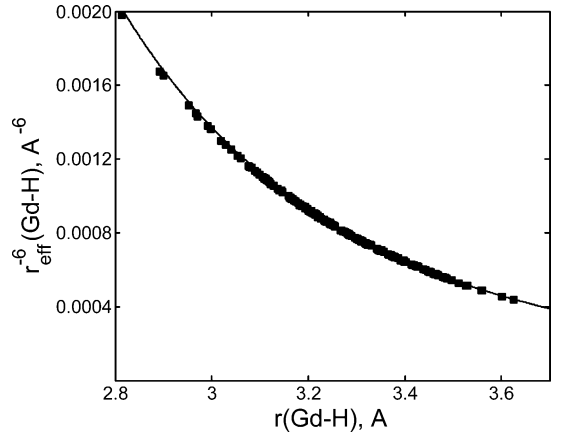

Figure 7. The r_{eff}^{-6}(Gd−H) factor for the hydrogen atom of bound water in $[GdDOTA(H_2O)]^-$ obtained from eq 10 based on the calculated dipolar HFI tensors of the 100 MD "snapshots" (200 values totally). The line corresponds to r^{-6}(Gd−H) calculated using the point-dipole approximation.

is −0.04 ± 0.02 MHz. Regarding the slightly longer Gd−H average distance from the MD simulations ($r_{Gd-H} = 3.27$ Å compared to 3.1 Å from ENDOR) the agreement between calculated and experimental A_{iso}(H) is also very satisfactory.

Anisotropic Hyperfine Coupling Constants of ^{17}O and ^{1}H in $[Gd(DOTA)(H_2O)]^-$. The results of anisotropic HFCCs are expressed in terms of effective distances of dipole−dipole interactions, r_{eff} (eq 5), for the reader's benefit and better understanding. It will furthermore allow us to compare the results of the calculations with those obtained within the point-dipole approximation. Figures 6 and 7 show the values of the r_{eff}^{-6} factor as function of the Gd−ligand nucleus distances. The values of r_{eff}^{-6}, obtained from eq 10, are based on the calculated dipolar HFI tensors for 100 MD snapshots. The point-dipole approximation used in the SBM equations uses internuclear distances r_{Gd-X}, and the corresponding factors r_{Gd-X}^{-6} are shown as solid lines in Figures 6 and 7.

From Figure 6 it can be seen that for ^{17}O the point-dipole approximation significantly overestimates the dipolar interaction between the ligand nuclear spin and the electron spin of the ion: The expectation value of the effective distance factor for dipolar relaxation is $\langle r_{eff}^{-6}(Gd-O)\rangle = 2.51 \times 10^{-3}$ Å^{-6} compared to the internuclear gadolinium−oxygen distance of $\langle r^{-6}(Gd-O)\rangle = 3.64 \times 10^{-3}$ Å^{-6}. This corresponds to the following average distances of dipole−dipole magnetic interac-

tions: $\langle r_{\mathrm{eff}}(\mathrm{Gd-O})\rangle = 2.72$ Å and $\langle r(\mathrm{Gd-O})\rangle = 2.56$ Å, respectively. Neglecting spin-polarization effects leads therefore to an overestimation of the dipolar ^{17}O nuclear spin relaxation rates by approximately 45%.

The point-dipole approximation is however valid to describe the anisotropic HFI between Gd^{3+} and ^{1}H of the inner sphere water molecule in $[Gd(DOTA)(H_2O)]^-$. From Figure 7 one can note that $r_{\mathrm{eff}}{}^{-6}(\mathrm{Gd-H})$ deviates only very slightly from $r^{-6}(\mathrm{Gd-H})$ at short Gd−H distances and the average values are virtually identical: $\langle r_{\mathrm{eff}}{}^{-6}(\mathrm{Gd-H})\rangle = 8.48 \times 10^{-4}$ Å^{-6} and $\langle r^{-6}(\mathrm{Gd-H})\rangle = 8.56 \times 10^{-4}$ Å^{-6}.

Conclusions

The study of physicochemical parameters of gadolinium based MRI contrast agents is to a large extent based on ^{1}H and ^{17}O NMR relaxation measurements. The strong interaction between the nuclear spins and the electron spin of Gd^{3+} dominates the relaxation properties and allows the determination of rotational correlation times and water exchange rates, for example. Thus, an accurate knowledge of the isotropic and anisotropic parts of the hyperfine coupling constant is imperative for an accurate assessment of the data.

Our quantum chemical investigation of hyperfine coupling constants between Gd^{3+} ion and bound water molecules shows that the ^{1}H isotropic hyperfine coupling constants, A_{iso}, are small. Thus, the contribution of scalar relaxation to the relaxation enhancement can therefore be safely neglected as it has already been deduced from experimental data. What is more essential, the evaluation of the anisotropic part of the **A**-tensor shows that the point-dipole approximation is valid for ^{1}H NMR of bound water molecules. The distance $r_{\mathrm{Gd-H}}$ introduced in SBM theory can therefore be safely set to the distance between the gadolinium and the proton nuclei.

Reduced transverse ^{17}O NMR relaxation rates $1/T_{2\mathrm{r}}$ are, in the case of Gd-based complexes, dominated by the scalar relaxation mechanism which depends on A_{iso}. This isotropic hyperfine coupling constant can be best determined experimentally by ^{17}O NMR shift measurements. Our calculated A_{iso}(O) strongly correlates with the metal−oxygen distance, and therefore, NMR shift measurements give at least a qualitative indication for $r_{\mathrm{Gd-O}}$: smaller coupling constants are indicative for longer Gd−O distances.

Reduced longitudinal ^{17}O NMR relaxation rates, $1/T_{1\mathrm{r}}$, are controlled to about two-thirds by the dipolar contribution, $1/T_1^{\mathrm{DD}}$, and to about one-third by the quadrupolar contribution, $1/T_1^{\mathrm{Q}}$.[3] The quantum chemical evaluation of the anisotropic HFI tensor **T** has shown that spin-polarization effects play an essential role for proper evaluation of ^{17}O HFI tensor. The point-dipole approximation, based on internuclear distances, significantly overestimates the interaction between electron and ^{17}O-nuclear spin. To compensate for the 45% decrease of $1/T_1^{\mathrm{DD}}$ by using the correct distance for dipolar interaction (2.72 Å instead of 2.46 Å) a ∼25% increase of the rotational correlation time τ_{R} is needed.

Acknowledgment. We thank Dr. Alain Borel for helpful discussions. The Swiss National Science Foundation is acknowledged for financial support. Work in Bratislava has been supported by the Slovak Grant Agencies VEGA (No. 2/3103/23) APVT (No. 51-045502), EURATOM FP6 Integrated Project (FUNMIG), and European COST D18 action "Lanthanide Chemistry for Diagnosis and Therapy". This research was carried out in the frame of the European-funded EMIL program (LSHC -2004 - 503569).

Supporting Information Available: Tables with geometry of Gd aqua complex and GTO basis sets. This material is available free of charge via the Internet at http://pubs.acs.org.

References and Notes

(1) Bertini, I.; Lee, Y.-M.; Luchinat, C.; Piccioli, M.; Poggi, L. *ChemBioChem* **2001**, *2*, 550−558.
(2) Tóth, É.; Helm, L.; Merbach, A. E. In *Topics in Current Chemistry*; Krause, W., Ed.; Spinger-Verlag: Berlin, 2002; Vol. 221, pp 62−101.
(3) Tóth, É.; Helm, L.; Merbach, A. E. In *The Chemistry of Contrast Agents in Medical Magnetic Resonance Imaging*; Tóth, É., Merbach, A. E., Eds.; Wiley: Chichester, 2001.
(4) Helm, L.; Toth, E.; Merbach, A. E. Lanthanide ions as magnetic resonance imaging agents. Nuclear and electronic relaxation properties. Applications. In *The Lanthanides and Their Interrelations with Biosystems*; Metal Ions in Biological Systems; Sigel, A., Sigel, H., Eds.; ; M. Dekker: New York, 2003; Vol. 40, pp 589−641.
(5) Tóth, É.; Helm, L.; Merbach, A. E. In *Comprehensive Coordination Chemistry II*; McCleverty, J. A., Meyer, T. J., Eds.; Elsevier: Oxford, U.K., 2004; Vol. 9, pp 841−881.
(6) Caravan, P.; Ellison, J. J.; McMurry, T. J.; Lauffer, R. B. *Chem. Rev.* **1999**, *99*, 2293−2352.
(7) Bertini, I.; Luchinat, C.; Parigi, G. *Concepts Magn. Reson.* **2002**, *14*, 259−286.
(8) Allegrozzi, M.; Bertini, I.; Janik, M. B. L.; Lee, Y.-M.; Liu, G.; Luchinat, C. *J. Am. Chem. Soc.* **2000**, *122*, 4154−4161.
(9) Pintacuda, G.; Otting, G. *J. Am. Chem. Soc.* **2002**, *124*, 372−373.
(10) Aime, S.; D'Amelio, N.; Fragai, M.; Lee, Y.-M.; Luchinat, C.; Terreno, E.; Valensin, G. *J. Biol. Inorg. Chem.* **2002**, *7*, 617−622.
(11) Iwahara, J.; Schwieters, C. D.; Clore, G. M. *J. Am. Chem. Soc.* **2004**, *126*, 5879−5896.
(12) Fields, R. A.; Hutchison, C. A. J. *J. Chem. Phys.* **1985**, *82*, 1711−1722.
(13) Caravan, P.; Astashkin, A. V.; Raitsimring, A. M. *Inorg. Chem.* **2003**, *42*, 3972−3974.
(14) Solomon, I. *Phys. Rev.* **1955**, *99*, 559−565.
(15) Solomon, I.; Bloembergen, N. *J. Chem. Phys.* **1956**, *25*, 261−266.
(16) Bloembergen, N. *J. Chem. Phys.* **1957**, *27*, 572−573.
(17) Bloembergen, N.; Morgan, L. O. *J. Chem. Phys.* **1961**, *34*, 842−850.
(18) Kowalewski, J.; Laaksonen, A.; Nordenskiöld, L.; Blomberg, M. *J. Chem. Phys.* **1981**, *74*, 2927−2930.
(19) Nordenskiöld, L.; Laaksonen, A.; Kowalewski, J. *J. Am. Chem. Soc.* **1982**, *104*, 379−382.
(20) Kowalewski, J.; Nordenskiöld, L.; Benetis, N.; Westlund, P.-O. *Prog. NMR Spectrosc.* **1985**, *17*, 141−185.
(21) Sahoo, N.; Das, T. P. *J. Chem. Phys.* **1989**, *91*, 7740−7748.
(22) Sahoo, N.; Das, T. P. *J. Chem. Phys.* **1990**, *93*, 1200−1208.
(23) Lata, K. R.; Sahoo, N.; Das, T. P. *J. Chem. Phys.* **1991**, *94*, 3715−3721.
(24) Wilkens, S. J.; Xia, B.; Volkman, B. F.; Weinhold, F.; Markley, J. L.; Westler, W. M. *J. Phys. Chem. B* **1998**, *102*, 8300−8305.
(25) Maron, L.; Eisenstein, O. *J. Phys. Chem. A* **2000**, *104*, 7140−7143.
(26) Kaupp, M., Bühl, M., Malkin, V. G., Eds. *Calculation of NMR and EPR parameters: Theory and Applications*; Wiley-VCH: Weinheim, 2004.
(27) Golding, R. M.; Pascual, R. O. *J. Magn. Res.* **1982**, *46*, 30−42.
(28) Glendening, E. D.; Petillo, P. A. *J. Phys. Chem. B* **2001**, *105*, 1489−1493.
(29) Improta, R.; Barone, V. *Chem. Rev.* **2004**, *104*, 1231−1253.
(30) Harriman, J. E. *Theoretical Foundation of Electron Spin Resonance*; Academic Press: New York, 1987; Vol. 37.
(31) Adamo, C.; Barone, V.; Subra, R. *Theor. Chem. Acc.* **2000**, *104*, 207−209.
(32) Weltner, W., Jr. *Magnetic Atoms and Molecules*; Dover Publication, Inc.: New York, 1989.
(33) Hansen, D. F.; Led, J. J. *J. Am. Chem. Soc.* **2004**, *126*, 1247−1252.
(34) Mispelter, J.; Momenteau, M.; Lhoste, J. In *Biological Magnetic Resonance: NMR of Paramagnetic* Molecules; Berliner, L. J., Reuben, J., Eds.; Plenum Press: New York, 1993; Vol. 12, pp 299−355.
(35) Gottlieb, H. P. W.; Barfield, M.; Doddrell, D. M. *J. Chem. Phys.* **1977**, *67*, 3785−3794.
(36) Borel, A.; Helm, L.; Daul, C. A. E. *Chem. Phys. Lett.* **2004**, *383*, 584−591.
(37) Ohtaki, H.; Radnai, T. *Chem. Rev.* **1993**, *93*, 1157−1204.
(38) Malkin, V. G.; Malkina, O. L.; Steinebrunner, G.; Huber, H. *Chem. Eur. J.* **1996**, *2*, 452−457.
(39) Eggenberger, R.; Gerber, S.; Huber, H.; Searles, D.; Welker, M. *J. Chem. Phys.* **1992**, *97*, 5898−5904.

(40) Eggenberger, R.; Gerber, S.; Huber, H.; Searles, D.; Welker, M. *J. Mol. Spectrosc.* **1992**, *151*, 474−481.
(41) Eggenberger, R.; Gerber, S.; Huber, H.; Searles, D.; Welker, M. *J. Comput. Chem.* **1993**, *14*, 1553−1560.
(42) Huber, H. *Z. Naturforsch.* **1993**, *49a*, 103−115.
(43) Takase, H.; Kikuchi, O. *Chem. Phys.* **1994**, *181*, 57−62.
(44) Asher, J. R.; Doltsinis, N. L.; Kaupp, M. *J. Am. Chem. Soc.* **2004**, *126*, 9854−9861.
(45) Jorgensen, W. L.; Chandrasekhar, J.; Madura, J. D. *J. Chem. Phys.* **1983**, *79*, 926−935.
(46) Case, D. A.; et al. *AMBER 6*; University of California: San Francisco, 1999.
(47) Borel, A.; Helm, L.; Merbach, A. E. *Chem. Eur. J.* **2001**, *7*, 600−610.
(48) Yerly, F.; Borel, A.; Helm, L.; Merbach, A. E. *Chem. Eur. J.* **2003**, *9*, 5468−5480.
(49) Aime, S.; Botta, M.; Fasano, M.; Marques, M. P. M.; Geraldes, C.; Pubanz, D.; Merbach, A. E. *Inorg. Chem.* **1997**, *36*, 2059.
(50) Pyykko, P. *Chem. Rev.* **1988**, *88*, 563−594.
(51) Cundari, T. R.; Stevens, W. J. *J. Chem. Phys* **1993**, *98*, 5555−5565.
(52) Dolg, M.; Stoll, H.; Savin, A.; Preuss, H. *Theor. Chim. Acta* **1989**, *75*, 173.
(53) Dolg, M.; Liu, W.; Kaldova, S. *Int. J. Quantum Chem.* **2000**, *76*, 359−370.
(54) Adamo, C.; Barone, V. *J. Comput. Chem.* **2000**, *21*, 1153−1166.
(55) With some RECPs we encountered severe problems with the SCF convergence. In other cases, our RECP calculations did not reproduce even the sign of spin-density on ligands. There is a definite need in better gadolinium RECPs for an accurate calculation of Fermi contact HFIs.
(56) Douglas, M.; Kroll, M. N. *Ann. Phys. (N.Y.)* **1974**, *82*, 89.
(57) Lenthe, E. v.; Baerends, E. J.; Snijders, J. G. *J. Chem. Phys.* **1993**, *99*, 4597−4610.
(58) Lenthe, E. v.; Baerends, E. J.; Snijders, J. G. *J. Chem. Phys.* **1994**, *101*, 9783−9792.
(59) Belanzoni, P.; Lenthe, E. v.; Baerends, E. J. *J. Chem. Phys.* **2001**, *114*, 4421−4433.
(60) Frisch, M. J.; et al. Gaussian 03, Revision C.01. Gaussian, Inc.: Wallingford, CT, 2004.
(61) Baerends, E. J.; Autschbach, J. A.; Bérces, A.; et al. ADF2003.01; SCM, Theoretical Chemistry, Vrije Universiteit: Amsterdam, The Netherlands.
(62) Neese, F. *J. Chem. Phys.* **2003**, *118*, 3939−38948.
(63) Remenyi, C.; Reviakine, R.; Arbuznikov, A. V.; Vaara, J.; Kaupp, M. *J. Phys. Chem. A* **2004**, *108*, 5026−5033.
(64) Munzarovà, M. L.; Kaupp, M. *J. Phys. Chem. A* **1999**, *103*, 9966−9983.
(65) Munzarovà, M. L.; Kubáček, P.; Kaupp, M. *J. Am. Chem. Soc.* **2000**, *122*, 11900−11913.
(66) Nakajima, T.; Hirao, K. *J. Chem. Phys.* **2002**, *116*, 8270−8275.
(67) Kutzelnigg, W.; Fleischer, U.; Schindler, M. In *The IGLO-Method: Ab-initio Calculation and Interpretation of NMR Chemical Shifts and Magnetic Susceptibilities*; Diehl, P., Fluck, E., Gunther, H., Kosfeld R., Seelig, J., Eds.; *NMR−Basic Principles and Progress*; Springer-Verlag: Heidelberg, 1990; Vol. 23.
(68) Chesnut, D. B.; Moore, K. D. *J. Comput. Chem.* **1989**, *10*, 648−659.
(69) Neese, F. *J. Phys. Chem. A* **2001**, *105*, 4290−4299.
(70) Becke, A. D. *Phys. Rev. A* **1988**, *38*, 3098−3100.
(71) Perdew, J. P.; Wang, Y. *Phys. Rev. B* **1992**, *45*, 13244−13249.
(72) Becke, A. D. *J. Chem. Phys.* **1993**, *98*, 5648−5652.
(73) The DKH2 results of HFCC were obtained without taking into account the so-called "picture-change" effect [Malkin I.; et al. *Chem. Phys. Lett.* **2004**, *396*, 268]. Though in general this effect is rather small for HFCC on light atoms our pilot calculations show that the HFCC on ^{17}O in this complex would be reduced by about 10%, thus further improving the agreement between DKH2 and ZORA results. The "picture-change" effect on the anisotropic hyperfine tensor in this complex is negligible.
(74) Micskei, K.; Powell, D. H.; Helm, L.; Brücher, E.; Merbach, A. E. *Magn. Reson. Chem.* **1993**, *31*, 1011.
(75) Powell, D. H.; Dhubhghaill, O. M. N.; Pubanz, D.; Helm, L.; Lebedev, Y. S.; Schlaepfer, W.; Merbach, A. E. *J. Am. Chem. Soc.* **1996**, *118*, 9333−9346.
(76) Reuben, J.; Fiat, D. *J. Chem. Phys.* **1969**, *51*, 4909−4917.
(77) Raitsimring, A. M.; Astashkin, A. V.; Baute, D.; Goldfarb, D.; Caravan, P. *J. Phys. Chem. A* **2004**, *108*, 7318−7323.
(78) Yazyev, O. V.; Tavernelli, I.; Helm, L.; Roethlisberger, U. *Phys. Rev. B* **2005**, *71*, 115110.
(79) Please note: There is some confusion about the sign of the ^{17}O isotropic HFCC in Gd^{3+} complexes. In contrast to recent experimental work the correct sign of $A_{iso} = A/h$ of a water molecule bound to Gd^{3+} is positive (corresponding to negative spin density at the point of nucleus), leading to a downfield shift of the ^{17}O resonance.
(80) DeBeer, R.; Biesboef, F.; Ormondt, D. V. *Physica B* **1976**, *83*, 314.
(81) Astashkin, A. V.; Raitsimring, A. M.; Caravan, P. *J. Phys. Chem. A* **2004**, *108*, 1990−2001.
(82) Bryden, C. C.; Reilley, C. N.; Desreux, J. F. *Anal. Chem.* **1981**, *53*, 1418.
(83) Chang, C. A.; Francesconi, L. C.; Malley, M. F.; Kumar, K.; Gougoutas, J. Z.; Tweedle, M. F.; Lee, D. W.; Wilson, L. J. *Inorg. Chem.* **1993**, *32*, 3501.
(84) Bénazeth, S.; Purans, J.; Chalbot, M.; Nguyen-van-Duong, M. K.; Louisette, N.; Keller, F.; Gaudemer, A. *Inorg. Chem.* **1998**, *37*, 3667.